

ture functions and the coupling constant entering in the basic quark, gluon diagrams. These calculations do, of course, suffer from the problem regarding the "soft" behavior of the basic QCD diagrams, discussed in this paper.

This work was supported in part by the University of Wisconsin Research Committee with funds granted by the Wisconsin Alumni Research Foundation, and in part by the U. S. Energy Research and Development Administration under Contract No. EY-76-C-02-0881, COO-881-11.

<sup>1</sup>M. Della Negra *et al.*, Nucl. Phys. **B127**, 1 (1977).

<sup>2</sup>R. P. Feynman, R. D. Field, and G. C. Fox, Nucl.

Phys. **B128**, 1 (1977).

<sup>3</sup>A cut is always necessary because of the divergence of the Møller cross section when  $\hat{t} \rightarrow 0$ .

<sup>4</sup>J. Ranft and G. Ranft, CERN Report No. TH.2363-CERN, 1977 (to be published).

<sup>5</sup>B. Alper *et al.*, Nucl. Phys. **B100**, 237 (1975).

<sup>6</sup>D. Antreasyan *et al.*, Phys. Rev. Lett. **38**, 112 (1977).

<sup>7</sup>The small difference in Fig. 1(a) between the hatched curve from Ref. 1 and dotted line (revised) is due to the improved numerical methods.

<sup>8</sup>This statement is correct for all the  $p_T$  dependence of interest.

<sup>9</sup>A. P. Contagouris, private communication.

<sup>10</sup>R. D. Field, California Institute of Technology Report No. CALT-68-633 (to be published).

<sup>11</sup>J. F. Owens, E. Reya, and M. Gluck, Florida State University Report No. FSU HEP 770907 (to be published).

## Heavy-Lepton Decay and the $A_1$ Resonance

J.-L. Basdevant

*Laboratoire de Physique Théorique et Hautes Energies, Université Pierre et Marie Curie, Paris, France*

and

E. L. Berger

*High Energy Physics Division, Argonne National Laboratory, Argonne, Illinois 60439*

(Received 12 January 1978)

We show that the observation of the  $A_1$  resonance in  $\tau$  decay agrees with diffractive  $A_1$  production and that it confirms our previous analysis of the diffractive data.

Recent observations<sup>1,2</sup> of a strong enhancement of the  $\rho\pi$  mass distribution near  $\rho\pi$  threshold in the decay of the heavy lepton  $\tau \rightarrow \nu_\tau \rho\pi$ , and their interpretation as evidence for the  $A_1$  resonance, raise the important question of the compatibility of these new observations with older data<sup>3</sup> on the  $A_1$  system obtained in diffractive hadronic production experiments. The peak observed in  $\tau$  decay has a mass  $M_{A_1} \sim 1150$  MeV and a width  $\Gamma \sim 200$ – $300$  MeV. On the other hand, in a recent paper<sup>4</sup> we showed that the diffractive data imply the existence of a "broad"  $A_1$  resonance,  $\Gamma \sim 400$  MeV, whose mass we could establish only within the bounds  $M_{A_1} = 1350 \pm 150$  MeV. In the hadronic data, this large uncertainty in the probable mass can be traced to various uncertainties in the theoretical analysis, including the parametrization of the Deck diffractive background, and to the relative paucity of the data. Based on the diffractive data alone, the parameters of our preferred solution are  $M_{A_1} = 1185$  MeV, and  $\Gamma = 395$  MeV (solution *E* of Ref. 4). These parameters are

those of the position of the second-sheet pole of the  $\rho\pi \rightarrow \rho\pi$  amplitude in Ref. 4.

The purpose of this Letter is to demonstrate that a careful analysis of the data from  $\tau$  decay leads to good agreement with the  $A_1$  resonance deduced from diffractive data, that the  $\tau$  data restrict the range of solutions obtained in our earlier work,<sup>4</sup> and that our preferred solution *E* of Ref. 4 provides a good representation of the  $\rho\pi$  mass distribution from  $\tau$  decay.

The diagram in Fig. 1 represents  $\tau$  decay. The

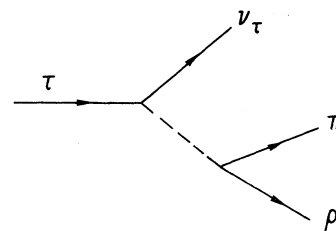


FIG. 1. Diagram for  $\tau$  decay.

corresponding amplitude is

$$\mathfrak{R} = l_\mu H_\mu, \quad (1)$$

where  $l_\mu$  is the usual lepton current  $\bar{u}_\nu \gamma_\mu (1 - \gamma_5) u_\tau$ . The hadronic axial-vector ( $J^P = 1^+$ ) current may be formed from the four-vectors  $\epsilon_\lambda^{(\rho)}$ , representing the polarization of the final  $\rho$ , and the momenta  $p^\rho$  and  $p^\pi$  of the final  $\rho$  and  $\pi$ , respectively. The most general form is

$$H_\mu = \left[ \epsilon_\mu^\rho - Q_\mu \frac{\epsilon^\rho \cdot p^\pi}{M^2} \right] F_1(M^2) + \epsilon^\rho \cdot p^\pi \left[ \Delta_\mu - Q_\mu \frac{m_\rho^2 - m_\pi^2}{M^2} \right] F_2(M^2), \quad (2)$$

where  $Q = p^\rho + p^\pi$ , and  $\Delta = p^\rho - p^\pi$ . The axial form factors  $F_1$  and  $F_2$  depend only on the  $\rho\pi$  invariant mass,  $M^2 = (p^\rho + p^\pi)^2$ . The relative size of  $F_1$  and  $F_2$  determines the proportion of the  $D$ -wave and  $S$ -wave contributions in  $A_1$  decay. In this article we set  $F_2 = 0$ , and retain only  $F_1$ . This corresponds to predominantly  $S$ -wave decay of the  $A_1$ , as is true of the hadronic data.<sup>3,4</sup> We also ignore absolute normalization (absolute decay rate).

After squaring Eq. (1) and summing over spins, we obtain a differential probability distribution for the decay:

$$\frac{d\mathcal{P}}{dM^2} \propto \int \sum |\mathfrak{R}|^2 \frac{d^3 p^\nu}{E_\nu} \frac{d^3 p^\rho}{E_\rho} \frac{d^3 p^\pi}{E_\pi} \delta(p^\tau - p^\nu - p^\rho - p^\pi) \delta(M^2 - (p^\rho + p^\pi)^2), \quad (3)$$

$$\sum |\mathfrak{R}|^2 = |F_1|^2 \left[ p^\tau \cdot p^\nu + \frac{2}{m_\rho^2} p^\tau \cdot p^\rho p^\nu \cdot p^\rho + \frac{2}{M^2} V_1 \cdot V_2 - \frac{V_1^2}{M^4} V_2 \cdot Q \right], \quad (4)$$

$$V_1 = p^\pi - p^\rho (p^\pi \cdot p^\rho) / m_\rho^2, \quad V_2 = m_\tau^2 p^\nu - m_\nu^2 p^\tau.$$

We compute the axial form factor  $F_1(M^2)$  using the standard formalism of final-state interactions<sup>5</sup> and the  $\rho\pi$  scattering amplitude derived in Ref. 4. Beginning with the  $2 \times 2$   $D$  matrix in Eq. (3.20) of Ref. 4, we find that  $F_1(M^2)$  is provided by the upper component of the vector

$$\begin{pmatrix} V_1 \\ V_2 \end{pmatrix} = D(M^2) \begin{pmatrix} \alpha + \beta M^2 \\ \gamma + \delta M^2 \end{pmatrix}; \quad (5)$$

that is,  $F_1(M^2) = V_1$ . The component  $V_2$  would yield the axial form factor for  $\tau \rightarrow \nu K^* \bar{K}$ . In Eq. (5),  $\alpha$ ,  $\beta$ ,  $\gamma$ , and  $\delta$  are arbitrary constants, in principle. They could be determined if one had enough statistics in  $\tau \rightarrow \nu \rho \pi$  (and in  $\tau \rightarrow \nu K^* \bar{K}$ ) to observe details of the  $M^2$  dependence. Such  $M^2$  dependence is not negligible in the pion electromagnetic form factor, for example.<sup>5</sup> Here we set

$$\alpha = 1, \quad \beta = \gamma = \delta = 0. \quad (6)$$

This is the simplest choice. Adding nonzero values of  $\beta$ ,  $\gamma$ , and  $\delta$  would only improve the fit we obtain. Our choice in Eq. (6) and our  $D$  matrix are such that our expressions reduce to the standard Omnès formula<sup>5</sup> in the simple case in which inelasticity is ignored in the form factor.

The mass distributions we obtain are compared with the data in Figs. 2 and 3. In Fig. 2 we show the results which emerge for two of the solutions reported in Ref. 4, solution  $E$  (preferred) with

$(M_{A_1}, \Gamma) = (1185 \text{ MeV}, 395 \text{ MeV})$ , and solution  $C$  with  $(M_{A_1}, \Gamma) = (1383 \text{ MeV}, 425 \text{ MeV})$ . Also shown in Fig. 2 is the distribution we obtain if we set  $F_1(M^2) = 1$ , retaining only the structure of the weak-interaction matrix element, without any  $\rho\pi$  interaction. In these calculations,  $m_\nu = 0$  and  $m_\tau = 1.9 \text{ GeV}$ . The curves in Figs. 2 and 3 for our solution  $E$  peak at  $M = 1180 \text{ MeV}$  and have a full

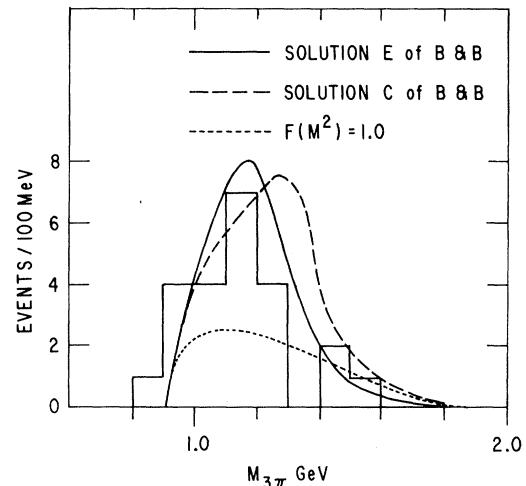


FIG. 2. Data from DORIS, Ref. 2. The solid curve is obtained from solution  $E$  of Ref. 4, as described in the text. The dashed curve represents solution  $C$ . The dotted curve results from retaining the weak-interaction matrix element alone, with  $F_1(M^2) = 1$ ,  $F_2 = 0$ . Normalizations of the theory curves are arbitrary.

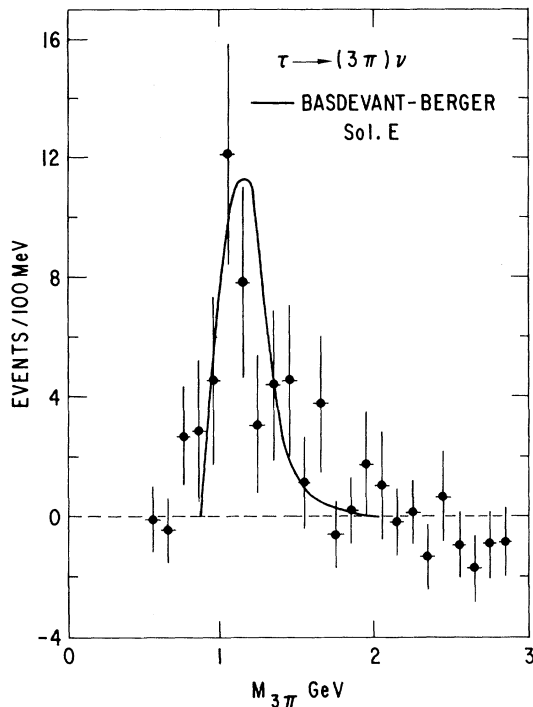


FIG. 3. Data from SPEAR, Ref. 1. The curve is obtained from solution E of Ref. 4.

width at half-maximum of  $\sim 320$  MeV.

A few obvious conclusions emerge from inspection of Figs. 2 and 3. (1) The preferred solution E of our fit to the diffractive data yields a good representation of the  $\rho\pi$  mass distribution in  $\tau$  decay. In this sense, there is complete agreement between the diffractive data on the  $A_1$  and the  $\tau$  decay results. The  $\tau$  data confirm our previous analysis of hadronic  $A_1$  production. (2) Our solution C, with  $M_{A_1} \sim 1385$  MeV does not agree with  $\tau$  decay. Therefore, the  $\tau$  data restrict the range of  $A_1$  mass parameters previously determined in fits to hadronic data. (3) It is unlikely that the  $\tau$  spectrum can be explained without an  $A_1$  resonance. For example, we tried varying the  $\nu_\tau$  mass, with  $F_1(M^2) = 1$ . Only for  $m_\nu$  as large as 400 or 600 MeV can a  $\rho\pi$  mass spectrum be obtained at all resembling the data. The results just reported above in (1) and (2) are insensitive to reasonable variations of  $m_\nu$ .

We have examined the changes which occur when we include nonzero values of  $F_2(M^2)$  in Eq. (2). For example, if we choose  $F_2/F_1$  such that the  $\rho\pi$  system is *purely* in an S wave, there are no appreciable differences from our results. However, if we retain only  $F_2$ , corresponding to  $D/S = -\sqrt{2}$ , then our  $A_1$  peak position is shifted

up by 90 MeV. Thus, our fit to the  $\tau$  data prefers a predominantly S-wave  $A_1$ , as in the hadronic data.<sup>3</sup>

A few technical remarks are perhaps in order. The reason that our calculated  $\rho\pi$  mass spectrum has a width narrower than the 394 MeV, which we quote for the  $A_1$  resonance, is that our resonance parameters are those of the second-sheet pole. For a very broad resonance, physical-region effects are distorted by phase-space factors and the like. The parameters of a broad resonance are difficult to establish from peak shapes alone. Second, it is an accident that the  $A_1$   $\rho\pi$  mass spectrum in  $\tau$  decay resembles the spectrum in diffractive production to the extent that it does. As shown in Ref. 4, the shape of the diffractive  $\rho\pi$  mass spectrum results from interference effects between the resonance and the unitarized Deck background. In  $\tau$  decay, the peak shape is determined by the rapid variation near threshold of phase space and of the weak-interaction matrix element, on which a broad, distorted Breit-Wigner amplitude is superimposed. We have not included "smearing" effects associated with the finite  $\rho$  width. This can be done with little trouble.

Finally, we comment on the absence of a significant  $A_1$  signal in charge-exchange reactions<sup>6</sup> such as  $\pi^- p \rightarrow (\rho\pi)^0 n$  and  $\pi^+ p \rightarrow (\rho\pi)^0 \Delta^{++}$ . This is a paradox which we do not pretend to understand completely. However, we are not altogether convinced by phenomenological estimates<sup>7</sup> of the expected  $A_1$  cross section in charge exchange since they are known to be very sensitive to the unknown  $D/S$  ratio in the  $A_1$  decay. (Changing  $D/S$  from  $-0.07$  to  $0$  reduces the estimated cross section by a factor of 20.) In addition, we speculate that the  $\rho$  exchange amplitude contains an additional suppression factor—vanishing near  $t_{\pi A_1} = 0$ . This guess is based on one of the conclusions of our study of diffractive production of the  $A_1$ . We found that the *direct* coupling of the Pomeron to the  $\pi A_1$  vertex is consistent with zero.<sup>4</sup> If  $f$  dominance of Pomeron couplings, or Pomeron- $f$  identity is invoked, then the direct  $f$  coupling is also expected to vanish. Next  $\rho$ - $f$  exchange degeneracy provides a zero in the direct  $\rho$  coupling. An additional zero of this type in the  $\rho$  residue function is also predicted along entirely different lines, from chiral-symmetry arguments.<sup>8</sup> Thus our view is that the  $A_1$  resonance is not seen in charge-exchange reactions, for perhaps good reasons, while it is observed clearly in  $\tau$  decay and in diffractive hadronic reactions.

To conclude, we believe we have established

the parameters of the  $A_1$  resonance:  $M_{A_1} = 1180 \pm 50$  MeV,  $\Gamma = 400 \pm 50$  MeV (second-sheet pole values). Moreover, we have fairly precise knowledge of the  $\rho\pi$  scattering amplitude itself. An interesting by-product is that we know the value of the axial-vector form factor, for which we provide an analytic parametrization.<sup>4,5</sup> This may be useful in various situations, for example, in tests of the second Weinberg sum rule.<sup>9</sup>

It is a pleasure to thank Professor Michel Gourdin for his interest and help, and Professor Leo Stodolsky and Dr. Cristian Sorenson for useful remarks. This work was supported in part by the United States Department of Energy. This work was performed under the auspices of the U. S. Department of Energy.

<sup>1</sup>J. A. Jaros *et al.*, SLAC Report No. SLAC-Pub-2084, 1978 (unpublished).

<sup>2</sup>G. Alexander *et al.*, Phys. Lett. **73B**, 99 (1978).

<sup>3</sup>Yu. M. Antipov *et al.*, Nucl. Phys. **B63**, 153 (1973); J. Pernegr *et al.*, to be published. Other recent data indicative of an  $A_1$  with low mass include P. Gavillet *et al.*, Phys. Lett. **69B**, 119 (1977); and A. Ferrer *et al.*, Orsay Report No. LAL 77/44, 1977 (unpublished).

<sup>4</sup>J.-L. Basdevant and E. L. Berger, Phys. Rev. D **16**, 657 (1977). For other approaches, see M. Bowler *et al.*, Nucl. Phys. **B97**, 227 (1975); R. S. Longacre and R. Aaron, Phys. Rev. Lett. **38**, 1509 (1977); R. Aaron *et al.*, Northeastern University Report NUB-2340, 1977 (unpublished).

<sup>5</sup>O. Babelon, J.-L. Basdevant, D. Cailleries, and G. Mennessier, Nucl. Phys. **B113**, 445 (1976), and references cited therein.

<sup>6</sup>C. Baltay *et al.*, Phys. Rev. Lett. **39**, 591 (1977); F. Wagner, M. Tabak, and D. M. Chew, Phys. Lett. **58B**, 201 (1975); M. J. Corden *et al.*, Rutherford Laboratory Report No. RL-77-139 A, 1977 (unpublished).

<sup>7</sup>G. C. Fox and A. J. G. Hey, Nucl. Phys. **B56**, 386 (1973); H. E. Haber and G. L. Kane, Nucl. Phys. **B129**, 429 (1977); A. Irving and V. Chaloupka, Nucl. Phys. **B89**, 345 (1975).

<sup>8</sup>L. R. Ram Mohan, Nucl. Phys. **B72**, 201 (1974).

<sup>9</sup>S. Weinberg, Phys. Rev. Lett. **18**, 507 (1967).

## Can Existing High-Transverse-Momentum Hadron Experiments Be Interpreted by Contemporary Quantum Chromodynamics Ideas?

R. D. Field

California Institute of Technology, Pasadena, California 91125

(Received 19 December 1977)

It is shown that if in a calculation of high-transverse-momentum meson production in hadron-hadron collisions one includes not only the scale-breaking effects that might be expected from asymptotically free theories but also the effects due to the transverse momentum of quarks in hadrons, *then* the results are not inconsistent with the single-particle cross-section data.

In previous papers (hereafter called FF1 and FFF<sup>1</sup>), experimental results on the production of high-transverse-momentum mesons have been analyzed. It was supposed that the phenomena were due to the hard scattering between quarks, one from the beam and one from the target.<sup>2</sup> The longitudinal momentum distribution of the quarks in the proton,  $G_{p \rightarrow q}(x)$ , and the distribution of mesons from the outgoing quarks,  $D_q^h(z)$ , were taken from data on lepton-initiated processes and assumed to scale (i.e., depend only on the fractional momentum  $z$  or  $x$  and not otherwise on energy). If these functions scale, then the invariant cross section for producing a large- $p_\perp$  meson directly reflects the energy dependence of the quark-quark cross section  $d\hat{\sigma}/d\hat{t}$ . Thus if the latter behaves as  $h(t/s)/s^n$ , then the former behaves as  $f(x_\perp, \theta_{c.m.})/p_\perp^{2n}$ , where  $x_\perp = 2p_\perp/W$  and  $W = \sqrt{s}$ . The expectation from field theories

calculated to any finite order using perturbation theory is that  $n \approx 2$ , whereas existing experimental data behave like  $1/p_\perp^3$  at fixed  $x_\perp$ . It appeared that if one wanted to describe existing data in terms of quarks, then  $d\hat{\sigma}/d\hat{t}$  would have to be modified to agree with experiment. The form  $d\hat{\sigma}/d\hat{t} = (2300 \text{ mb})/\hat{s}\hat{t}^3$  appeared to fit the large- $p_\perp$  meson data best.

This simple model (called the quark-quark scattering "black-box" model) succeeded in predicting the large- $p_\perp$   $\pi^+/\pi^-$  and  $K^+/K^-$  ratios. However, an analysis of the correlations between two or more particles produced at large  $p_\perp$  shows that effects due to the transverse-momentum distribution of the quarks in the initial hadrons,  $\langle k_\perp \rangle_{h \rightarrow q}$ , and the transverse momentum of the hadrons from the outgoing quark jets,  $\langle k_\perp \rangle_{q \rightarrow h}$ , cannot be neglected. In FFF  $\langle k_\perp \rangle_{h \rightarrow q} = 500$  MeV and  $\langle k_\perp \rangle_{q \rightarrow h} = 330$  MeV were used, but even these